Research paper

Application of a mathematical model to an artificial aquifer under different recharge/discharge conditions using 222Rn as a tracer

Santiago Celaya [a,b], Ismael Fuente [a,*], Daniel Rábago [a,b], Luis Quindós [a,b], Carlos Sainz [a,b]

[a] Radon Group, University of Cantabria, c/Cardenal Herrera Oria s/n, 39011, Santander, Spain
[b] The Cantabrian International Institute for Prehistoric Research (IIIPC), University of Cantabria, Avda de los Castros 52, 39005, Santander, Spain

HIGHLIGHTS

- Construction of an artificial aquifer with a source of water with 222Rn.
- Application of a mathematical model in waters that supply an artificial aquifer using 222Rn as a tracer.
- 11 simulations of Recharge and Discharge episodes in the artificial aquifer.
- Applied mathematical models: Closed Compartment Model (CCM) or Open Compartment Model (OCM).
- The results determine the origin of the water used in the recharge episodes.

GRAPHICAL ABSTRACT
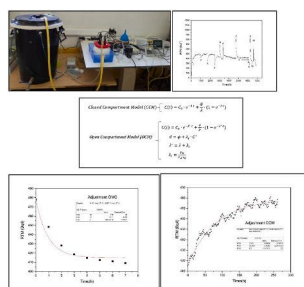
ARTICLE INFO

ABSTRACT

Radon (^{222}Rn), a radioactive gas of natural origin, was listed by the World Health Organization in 2009 as the second largest cause of lung cancer (3–14%) after tobacco. Global awareness of the importance of controlling its concentration in water led to the implementation of the European Directive 2013/51/Euratom, which establishes permitted levels in drinking water. This study applies a mathematical model to determine ^{222}Rn concentration in water supplying an artificial aquifer over the full range of recharge/discharge conditions (volumes and times, and therefore flows). This was done by creating an artificial aquifer on a laboratory scale, which reproduces the recharges and discharges experienced by real aquifers through rainwater or groundwater. The equipment used in this study was an RTM 2100 with a specific system for continuous monitoring of ^{222}Rn in water, a high-purity Ge detector for gamma spectrometry, and a portable liquid scintillation counter (LSC) called Triathler for specific measurements of ^{222}Rn in water. The aim of this paper is to show the application of the mathematical model under different recharge/discharge conditions applied to the artificial aquifer. The concentration of ^{222}Rn in water determined by the model can also be used as a tracer to find the origin and volume of water that reaches a real aquifer.
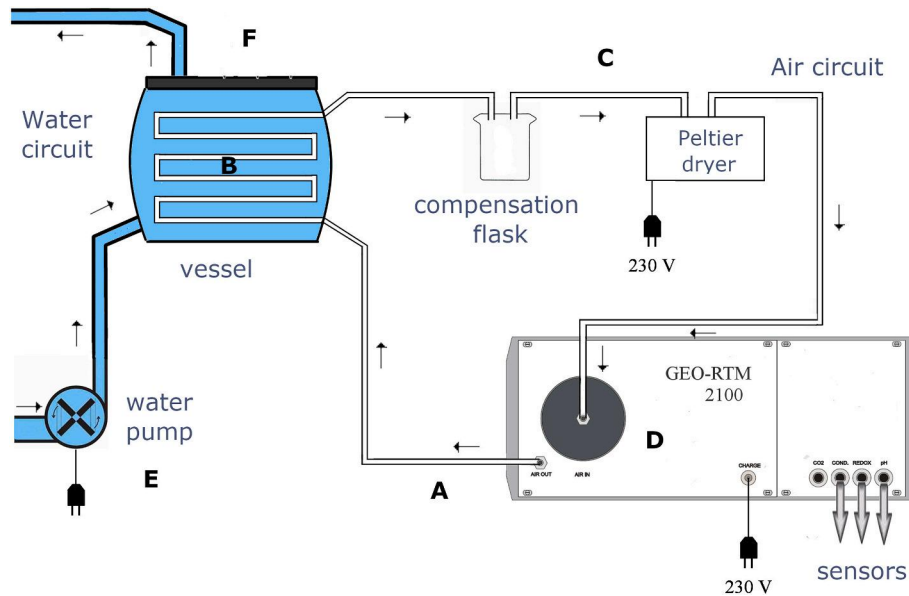
Fig. 1. Diagram of the system used to measure ^{222}Rn in water with an RTM 2100 (Sainz et al., 2016).

1. Introduction

The concentrations of ^{222}Rn that can be found in the outside air are practically negligible, with an annual average of 10 Bq·m^{-3} (Nero et al., 1990; WHO, 2001). However, in the inside of buildings and naturally enclosed spaces such as wells, galleries, or caves, the values can be very high, such as 50,462 Bq·m^{-3} in the cave of Castañar de Ibor (Lario et al., 2006), or quite high, such as the average value of 2500 Bq·m^{-3}, as shown in a study of 220 caves (Cigna, 2005). In general, its location in the ground coincides directly with the distribution of the parent (^{226}Ra, which through the emission of an α-particle in its decay process generates the nucleus of ^{222}Rn). This is, however, not always true, since in addition to molecular diffusion (short displacements through concentration gradients), there are air convective mechanisms (fast and significant displacements driven by pressure gradients), and it can also be carried far from the point of production by water.

Since it is a gas, existing studies mainly focused on determining its concentration in the air, in places such as underground mines (Youssef et al., 2019; Veiga et al., 2004), workplaces, and homes (Quindós, 1995; ICRP 137, 2017), but groundwater is also a very important route for the accumulation and transport of ^{222}Rn. Values in water can span from less than 2 Bq·l^{-1} in surface water up to 50,000 Bq•l^{-1} in groundwater (CSN, 2001; Haroon et al., 2022; Qasim et al., 2021), which occurs when water passes over rocks with a high content of ^{226}Ra or circulates through cracks with high concentrations of ^{222}Rn in the air. Some studies have shown that high levels of ^{222}Rn dissolved in water are a significant source in enclosed spaces and lead to non-negligible radiation in the gastrointestinal tract and throughout the body by means of ingestion (Galán et al., 2004).

Other research has used ^{222}Rn as a tracer to study water discharge in groundwater (Avery et al., 2018) and in submarine groundwater (Selvam et al., 2021), but other methodologies are used with water samples taken at given points in time. In this case, however, ^{222}Rn in water was continuously monitored.

For this study, an artificial aquifer with stable concentrations of ^{222}Rn was built in the laboratory, with the aim of validating a mathematical model under different recharge/discharge conditions, which happens in real aquifers such as in Las Caldas of the Besaya thermal spa, analysed by our research Group (Sainz et al., 2016). The experimentation in the laboratory is innovative in so far as it has allowed an artificial aquifer to be recharged with waters of different origin, simulating recharges with rainwater (^{222}Rn free) or with groundwater (rich in ^{222}Rn). It was further possible to work with different recharge and discharge conditions (different volumes, flows, ^{222}Rn concentrations and recharge and discharge times) (Celaya, 2018).

The main aim of this research is to validate a mathematical model that allows ^{222}Rn to be used as a tracer to determine the origin and volume of the water that reaches natural aquifers.

2. Materials and methods

2.1. Instrumentation

2.1.1. HPGe coaxial detector

The HPGe coaxial detector (model GL-2015-7500, Canberra, USA) allows the detection of gamma emissions between 30 and 3000 keV. ^{222}Rn concentration (Celaya et al., 2018b) was determined by the counts taken in the spectrum that correspond to ^{214}Pb (351.932 keV; Laboratoire National Henri Becquerel, 2018) with an efficiency of 1.29% and FWHM (Full Width Half Maximum) of 0.66%.

2.1.2. Triathler with alpha/beta separator (LSC)

We used a Triathler (model 425-034) with an integrated alpha/beta separator (Hidex, Finland) as the liquid scintillation counter (LSC). This instrument differentiates the longer pulse duration of alpha particles ($\simeq$ 100 ns) from the shorter pulse duration generated by beta particles ($<$30 ns) (Wisser et al., 2006).

This technique allows detecting generated alpha emissions in the disintegration of ^{226}Ra, ^{222}Rn, and its short-lived descendants (^{218}Po and ^{214}Po) through a photomultiplier tube. The liquid scintillator (Aqualight, Hidex) is a hydrocarbon with two aromatic rings called diisopropylnaphthalene, used in the so-called direct or one-phase method to measure ^{222}Rn in water (Celaya et al., 2018b).

The efficiency obtained was 262% when the sample contained ^{222}Rn (^{218}Po and ^{214}Po will also be generated) without the presence of ^{226}Ra, and 349% when the sample contained ^{226}Ra (^{222}Rn, ^{218}Po and ^{214}Po will also be generated). Calibration was performed using a certified source of ^{222}Ra and dilutions with various known concentrations (12, 20, 32, 100, 296, 843 and 2943 Bq·l^{-1}) (Celaya et al., 2018b).

The good results obtained with this instrument in national (Celaya et al., 2018a) and international intercomparison exercises for radon in water, such as REM 2018 (Joint Research Centre) or Proftest SYKE 2015
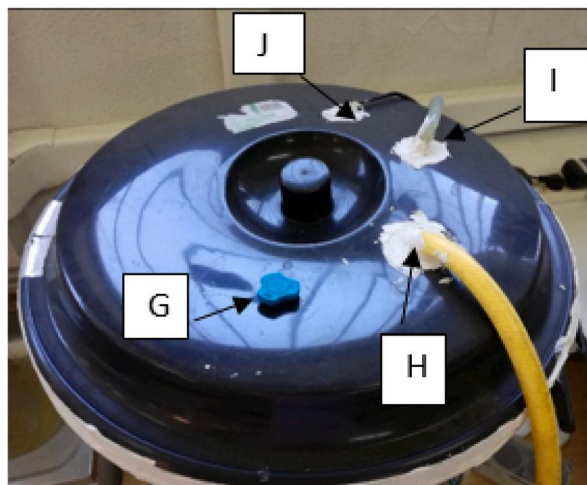
Fig. 2. Image of the lid used to cover the artificial aquifer.

(Finnish Environment Institute) confirm the correct calibration of this device.

2.1.3. RTM 2100

RTM 2100 (Sarad, Germany) is a device used for the continuous measurement of ^{222}Rn and ^{220}Rn concentration in air, as well as temperature, relative humidity, and atmospheric pressure. A pump inside drives air from the outside towards the 250 mm^3 measuring chamber, where a silicon detector is located, having previously passed through two filters that retain all descendants of ^{222}Rn and ^{220}Rn. The sensitivity of this equipment is 1.65 counts/(min·kBq·m^{-3}) according to the calibration certificate provided by Bundesamt Für Strahlenschutz (BFS).

Since this is a device that continuously measures ^{222}Rn in air, a system must be attached that allows continuous measurement in water. This system is based on the transfer of ^{222}Rn contained in water to the air that circulates through silicone tubes inside a container (Fig. 1). For this reason, it is necessary to calculate a transfer factor (t_f) to convert the measurement taken by the RTM 2100 of radon in air (Bq•m^{-3}) to radon in water (Bq•l^{-1}).

Fig. 1 shows two circuits. The water circuit is gray (B, E and F) while the air circuit is white (A, C y D). An internal pump starts the circuit; the air outlet is marked on the device with the designation "OUT" (A). The circuit continues with silicone tubes (B), which are impermeable to water but permeable to radon. This component is submerged and placed inside the container filled with the water to be measured. Next, there is a compensation bottle and a Peltier dryer (C), which prevent water vapour from entering the detector before the air returns to the equipment at the entrance marked "IN" (D). The other part of the system, i.e., the water circuit, begins with an external pump submerged in the aquifer (E). Its function is to continuously send water to the container (F) where the silicone tubes (B) are placed, and finally, the water returns to the aquifer container.

2.2. Artificial aquifer description

2.2.1. Aquifer container

To reproduce the recharge and discharge processes experienced by natural aquifers, an artificial aquifer was built on a laboratory scale. The first step was choosing the 100 l container.

A tap was incorporated into the structure to make the sampling accessible and acrylic putty was used to seal the lid and to serve as an insulator preventing water and ^{222}Rn from leaking.

From the top of the container lid (Fig. 2), the different tubes and perforations made for adaptation can be seen, as described below. Firstly, we can see the blue plug (G) with the hole where the aquifer
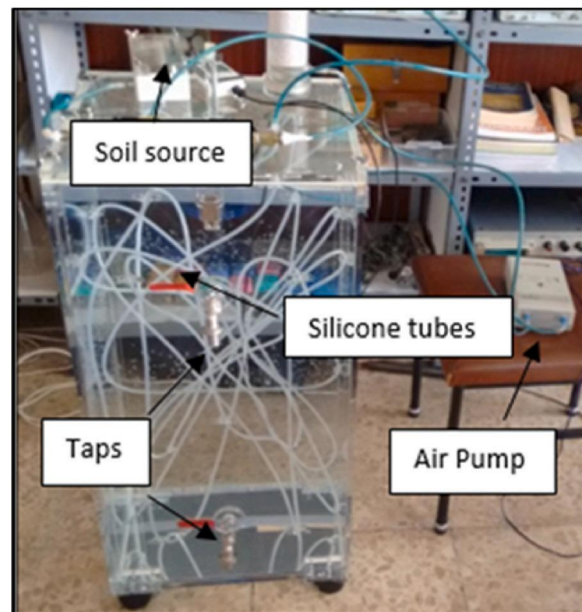

Fig. 3. Artificial generation of radon in water.

recharges. Next, the hose returning from the water circuit (H) and the outlet hose of the artificial aquifer identified by the transparent tube (I) can be seen. Finally, in the upper middle part is the electrical connection cable of the pump (J) which drives the water through the water circuit.

2.2.2. ^{222}Rn source of the artificial aquifer

Creating the ^{222}Rn source of the artificial aquifer relied on the expertise of our research group to construct a ^{222}Rn enriched water container with a source of ^{226}Ra (Fig. 3; Celaya et al., 2018b). Fig. 3 shows the distribution of the silicone tubes inside the methacrylate container used in the construction of the artificial aquifer. The aim is to distribute the silicone tubes throughout the container to ensure that ^{222}Rn is distributed homogeneously, thanks to a small pump that generates a current to mix the water.

The ^{222}Rn source was a methacrylate box containing uranium mine soil with ^{226}Ra (745 $\pm$ 20 kBq•kg^{-1} measured with a HPGe coaxial detector gamma spectrometer with Laboratory accreditation ISO 17025) that provided enough ^{222}Rn to achieve a concentration in water of 578 $\pm$ 28 Bq·l^{-1}. This box was connected by plastic tubes to a pump that applied a flow of 0.03 l min^{-1} of air, distributing the ^{222}Rn along the silicone tubes and then to the water.

Using the process described for the distribution of ^{222}Rn in the methacrylate container, 945 cm of silicone tubes were placed inside the artificial aquifer container attached to the radon source formed by 271 g of soil used in the previous experiment. The system that generates ^{222}Rn in the artificial aquifer is formed by a methacrylate box 8 × 16 × 5.5 cm (length x width x height) and 2 tubes. There is one inlet tube on the right side with air, which is driven by the pump, and another outlet tube on the left, which is joined to the silicone tubes inside the aquifer. The pump supplies an airflow of 0.03 l min^{-1}, which is sufficient to carry the air with ^{222}Rn generated in the box and to return it after passing through the silicone tubes inside the aquifer.

2.2.3. ^{222}Rn source to generate the radon-rich recharge water

The system was developed to generate groundwater rich in ^{222}Rn, which is used to recharge the artificial aquifer. A cooling box was loaded with water from a public supply, inside a glass bowl containing soil rich in ^{226}Ra (745 $\pm$ 20 kBq•kg^{-1}) was placed and sealed with an elastic silicone lid in order to diffuse ^{222}Rn easily into the water.
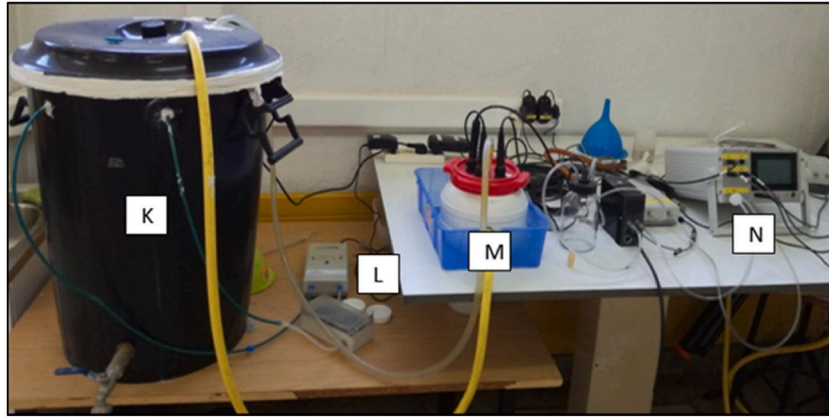
Fig. 4. Complete structure of the artificial aquifer.

2.3. Sample collection

Water sampling in the artificial aquifer was carried out through the tap, with each sample collected in 100 ml beakers. The process consisted of putting the tap next to the beaker and taking 29 samples with a small flow of water. The aim was to avoid bubbles and splashes that could cause leaks of the content with ^{222}Rn and to measure them in the LSC in order to calculate the transfer factor (t_f).

2.4. Starting the artificial aquifer

Fig. 4 shows the complete structure of the artificial aquifer with all the described components. On the left, the aquifer container (K) can be seen. It is connected to the ^{222}Rn source (L) and to the RTM 2100 (N) measurement tool for ^{222}Rn in water (M).

To start it, the upper part was filled with approximately 100 l of water using a hose connected to a public water supply. After this initial charge, the RTM began the measuring process in the artificial aquifer, and 42 days later, the value of ^{222}Rn in the aquifer water reached equilibrium and the RTM measurements showed values of around $2.5 \cdot 10^6$ Bq·m^{-3}.

2.4.1. Transfer factor calculation

This factor is necessary to convert the values of radon in air (Bq·m^{-3}) of the RTM 2100 to the values of radon in water (Bq·l^{-1}). To calculate this factor, 29 water samples were taken and measured with the LSC (Triathler), while the measurements provided by the RTM were being recorded in the meantime. The relationship between the RTM readings and the LSC (t_f) was obtained after applying a linear adjustment of type y = a*x.

The t_f factor, which is the slope obtained from this linear adjustment, allows the RTM 2100 readings expressed in Bq·m^{-3} to be converted into Bq·l^{-1} via Eq. (1).

$$C_{Rn}(LSC) = t_f \cdot C_{Rn}(RTM) \Rightarrow t_f = (1.98 \pm 0.01) \cdot 10^{-4} \frac{Bq \cdot l^{-1}}{Bq \cdot m^{-3}} \tag{1}$$

2.5. Mathematical models

The mathematical models used in this study can explain the variation experienced by the concentration of ^{222}Rn in the aquifer during the recharge and discharge processes that take place continuously. There are two models that are applied in the possible states of the aquifer (Saínz et al., 2016).

2.5.1. Closed Compartment Model (CCM)

This model attempts to explain the variation in the concentration of ^{222}Rn over time when the aquifer has no external water supply, i.e.,

when it maintains a constant volume. The differential equation that explains this situation is Eq. (2) (Kowalczk et al., 2010; Sainz et al., 2016):

$$\frac{dC}{dt} = \varphi - \lambda \cdot C \tag{2}$$

Solving this differential equation allows the dynamics of the ^{222}Rn concentration in water in a CCM to be determined.

$$C(t) = C_0 \cdot e^{-\lambda \cdot t} + \frac{\varphi}{\lambda} \cdot (1 - e^{-\lambda \cdot t}) \tag{3}$$

To understand the terms of Eq. (3), it is necessary to look at Eqs. (4) and (5):

$$\varphi = \frac{E \cdot S}{V} \tag{4}$$

$$\lambda = \lambda_{Rn} + \lambda_v \tag{5}$$

where:

  i) $C(t)$ is the ^{222}Rn concentration in water over time (Bq•l^{-1}).
 ii) C_0 is the initial ^{222}Rn concentration in water (Bq•l^{-1}).
iii) λ is the constant that adds the λ_{Rn} and the λ_v (h^{-1}).
 iv) λ_{Rn} is the ^{222}Rn decay constant, $7.55 \cdot 10^{-3}$ h^{-1} ($\lambda_{Rn} = \ln(2)/T_{1/2}$, (Laboratoire National Henri Becquerel, 2018).
  v) λ_v is the constant that reflects ^{222}Rn loss at the water-air interface per unit time (h^{-1}).
 vi) t is time (h).
vii) φ is the radon emission rate for the aquifer source (Bq•l^{-1}·h^{-1}).
viii) E is the ^{222}Rn exhalation for the aquifer source (Bq•h^{-1}·m^{-2}).
 ix) S is the exhalation surface of the aquifer source (m^2).
  x) V is the volume of water (l).

2.5.2. Open Compartment Model (OCM)

The need to model aquifers that have external water contributions with different ^{222}Rn concentrations leads to adapting the previous model (CCM) to the Open Compartment Model (OCM). This new model assumes the previous terms, except for the addition of a new exchange term. The differential equation that expresses this mathematical model is (Kowalczk et al., 2010; Sainz et al., 2016):

$$\frac{dC}{dt} = \varphi - \lambda \cdot C - \lambda_I \cdot (C - C^*) \tag{6}$$

Solving this differential equation allows the dynamics of the ^{222}Rn concentration in water in an OCM to be determined.

$$C(t) = C_0 \cdot e^{-\lambda^* \cdot t} + \frac{d}{\lambda^*} \cdot (1 - e^{-\lambda^* \cdot t}) \tag{7}$$

Table 1

Specifications of the 11 simulations performed in the artificial aquifer.

Simulation	Recharge				Discharge			Specifications	
	C_R	t_R	V_R	Q_R	t_D	V_D	Q_D		
1	Initial charge and ^{222}Rn growth of the artificial aquifer								
2	$< L_D$	10	14.4	86.4	5	14.4	172.8	$Q_R \neq Q_D$	$V_A \neq$ cst
3	$< L_D$	25	31.3	75.1	10	31.3	187.8	$Q_R \neq Q_D$	$V_A \neq$ cst
4	$< L_D$	60	50.0	50.0	15	50.0	200.0	$Q_R \neq Q_D$	$V_A \neq$ cst
5	2109 ± 88	10	16.6	99.6	5	16.6	199.2	$Q_R \neq Q_D$	$V_A \neq$ cst
6	1805 ± 76	10	16.6	99.6	5	16.6	199.2	$Q_R \neq Q_D$	$V_A \neq$ cst
7	2191 ± 91	45	44.0	58.7	15	44.0	176.0	$Q_R \neq Q_D$	$V_A \neq$ cst
8	$< L_D$	300	24.0	4.8	10	24.0	144.0	$Q_R \neq Q_D$	$V_A \neq$ cst
9	3340 ± 136	300	24.0	4.8	10	24.0	144.0	$Q_R \neq Q_D$	$V_A \neq$ cst
10	$< L_D$	425	24.0	3.4	425	24.0	3.4	$Q_R = Q_D$	$V_A =$ cst
11	3313 ± 135	400	24.0	3.6	400	24.0	3.6	$Q_R = Q_D$	$V_A =$ cst

C_R, ^{222}Rn concentration in recharge water (Bq·l^{-1}); t_R, time of recharge (min); V_R, volume of recharge (l); Q_R, flow of de recharge (l·h^{-1}); t_D, time of discharge (min); V_D, volume of discharge (l); Q_D, flow of discharge (l·h^{-1}); V_A, volume of the artificial aquifer (l); cst, constant; L_D, detection limit of LSC is 2 Bq•l^{-1}.
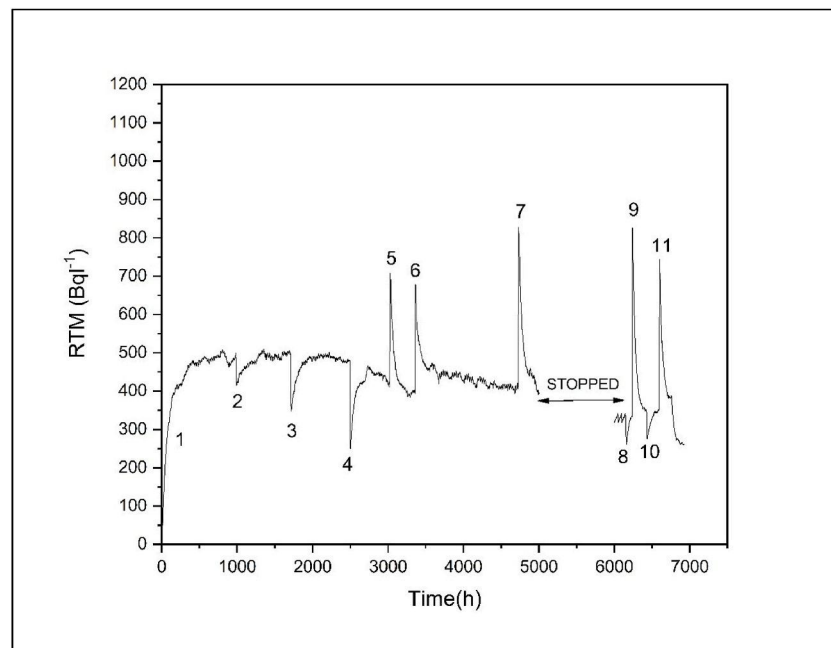

Fig. 5. General graph of ^{222}Rn concentration in the artificial aquifer with the 11 performed simulations.

To understand the terms of Eq. (7), it is necessary to look at Eqs. (8)–(10):

$$d = \varphi + \lambda_I \cdot C^* \tag{8}$$

$$\lambda^* = \lambda + \lambda_I \tag{9}$$

$$\lambda_I = \frac{V_R}{V_A \cdot t_R} \tag{10}$$

where:

i) λ^* is a term that results from adding the λ calculated in the CCM and the λ_I of the volume exchange (h^{-1}).

ii) d is a term that adds the radon emission rate of the aquifer source and the radon concentration in recharge water multiplied by λ_I (Bq·l^{-1}·h^{-1}).

iii) λ_I is the constant that reflects the exchange of volume of water per unit time (h^{-1}).

iv) C^* is the ^{222}Rn concentration of the recharge water (Bq•l^{-1}).

v) V_R is the volume of water used in the recharge (l).

vi) V_A is the volume of the aquifer (l).

The aim of this mathematical model is to determine the concentration of ^{222}Rn in the recharge water of the aquifer, which is determined by C^*.

2.6. Simulations of recharge and discharge episodes in the artificial aquifer

Every simulation performed in this study has two parts: a recharge episode together with a discharge episode in order not to exceed the total volume of the artificial aquifer, around 100 l. Water discharges in this research simulate those of any aquifer to a river, sea or other nearby aquifer. The water discharged in the simulations was taken from the aquifer container tap and its volume was then measured. Likewise, the volumes of water used in the recharge episodes were measured both in the simulations with rainwater, in which water from the public supply (free of ^{222}Rn) was used, and in the simulations with groundwater in which enriched water sourced from the cooling box was used. Table 1 shows the 11 simulations carried out, and their specifications.
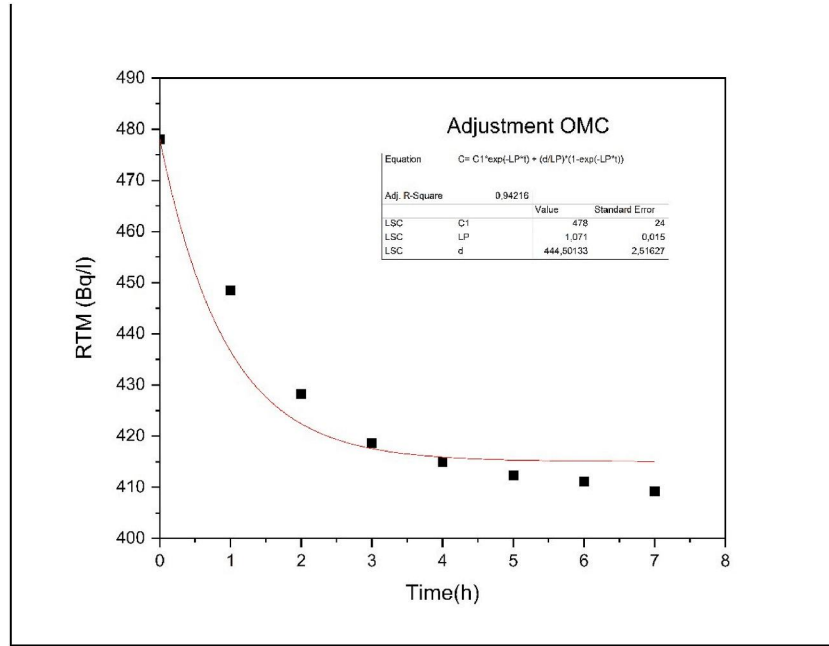
Fig. 6. Simulation 2: Decrease after the recharge with water from a public supply.
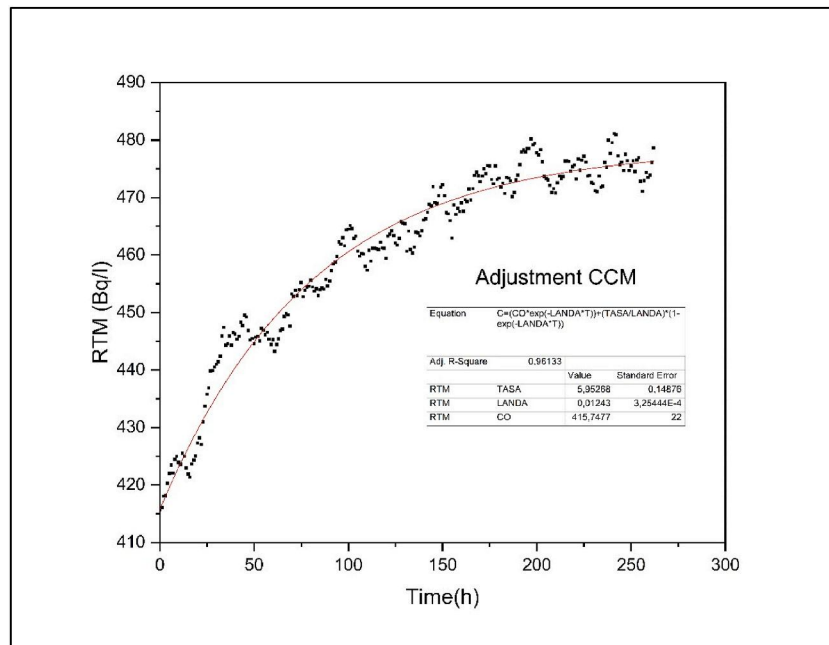

Fig. 7. Simulation 2: Increase after the recharge with water from a public supply.

Fig. 5 shows the general graph with the 11 discharge and recharge simulations carried out during the 15 months that the artificial aquifer was being studied. The line represents the ^{222}Rn concentration in Bq•l^{-1} measured by RTM 2100 after applying the t_f calculated from Eq. (1).

3. Results

Fig. 6 shows simulation 2, where the adjustment with OCM is made after the recharge with water from a public supply. It was observed that the concentration of ^{222}Rn in the water decreases for 7–8 h and begins to increase again until reaching equilibrium after 250–300 h. This increase can be seen in Fig. 7, where it begins to reach equilibrium at 250 h, applying the adjustment with CCM to the represented data. These

adjustments (OCM and CCM) made to simulation 2 have been applied to the 11 episodes, and the results of the adjustments are presented in Table 2.

Table 2 shows all the parameters of interest affected by applying the CCM and OCM mathematical models to the 11 recharge and discharge simulations performed in the artificial aquifer. Table 3, meanwhile, shows λ_I (Eq. (9)), λv (Eq. (5)), ^{222}Rn concentration measured with LSC (C_R) and ^{222}Rn concentration estimated with the model for the recharge water ($C*$).

As can be seen in the results of Table 3, simulations 2, 3 and 4, with water from a public supply and simulating the recharge of the aquifer with rainwater (^{222}Rn free), returned ^{222}Rn concentrations in the recharge water ($C*$) higher than the real concentrations (C_R) measured

Table 2
Results of the CCM and OCM models applied in the 11 simulations.

Simulation	CCM				OCM			
	C_o	φ	$\lambda \cdot (10^{-4})$	R^2	C_o	d	λ^*	R^2
1	$<L_D$	5.2 ± 0.1	110 ± 1	0.978				
2	416 ± 22	6.0 ± 0.2	120 ± 3	0.961	478 ± 24	445 ± 3	1.071 ± 0.015	0.94
3	347 ± 19	6.3 ± 0.1	130 ± 1	0.988	490 ± 25	420 ± 8	1.174 ± 0.016	0.87
4	253 ± 15	7.4 ± 0.1	170 ± 2	0.965	470 ± 24	294 ± 13	1.104 ± 0.015	0.86
5	696 ± 33	9.7 ± 0.1	240 ± 2	0.996	431 ± 22	883 ± 9	1.278 ± 0.018	0.96
6	677 ± 32	10.0 ± 0.2	220 ± 4	0.954	468 ± 24	855 ± 5	1.276 ± 0.018	0.98
7	815 ± 37	10.8 ± 0.1	250 ± 2	0.997	415 ± 22	926 ± 17	1.153 ± 0.016	0.94
8	219 ± 13	7.0 ± 0.5	230 ± 20	0.975	279 ± 16	14 ± 1	0.090 ± 0.002	0.96
9	689 ± 32	9.0 ± 0.1	300 ± 2	0.997	278 ± 16	136 ± 6	0.097 ± 0.001	0.96
10	230 ± 14	5.1 ± 0.4	170 ± 15	0.991	287 ± 16	8 ± 1	0.064 ± 0.002	0.99
11	621 ± 30	6.0 ± 0.3	230 ± 8	0.933	304 ± 17	107 ± 6	0.073 ± 0.001	0.96

C_o, initial concentration of ^{222}Rn (Bq·l^{-1}); φ, radon emission rate in CCM model (Bq·l^{-1}h^{-1}); λ, constant that reflects the ^{222}Rn loss in CCM model (h^{-1}); R^2, R-square; d, radon emission rate in OCM model (Bq·l^{-1}·h^{-1}); λ^*, constant that reflects the ^{222}Rn loss in OCM model (h^{-1}); L_D, detection limit of LSC is 2 Bq·l^{-1}.

Table 3
Simulation results after adjusting the CCM models y OCM.

Simulation	$\lambda_v \cdot (10^{-4})$	λ_I	C^*	C_R
1	Initial recharge			
2	40 ± 3.3	1.059 ± 0.015	415 ± 18	$< L_D$
3	50 ± 1.0	1.161 ± 0.016	356 ± 17	$< L_D$
4	96 ± 2.4	1.087 ± 0.015	264 ± 17	$< L_D$
5	160 ± 1.7	1.254 ± 0.018	696 ± 31	2109 ± 88
6	140 ± 4.2	1.254 ± 0.018	673 ± 30	1805 ± 76
7	170 ± 1.9	1.128 ± 0.016	812 ± 38	2191 ± 91
8	150 ± 20.0	0.066 ± 0.001	106 ± 17	$< L_D$
9	220 ± 2.3	0.066 ± 0.001	1924 ± 124	3340 ± 136
10	90 ± 15.0	0.047 ± 0.001	62 ± 23	$<L_D$
11	150 ± 8.0	0.050 ± 0.001	2020 ± 149	3313 ± 135

λ_v, is the constant that reflects ^{222}Rn loss in water-air interface per unit time (h^{-1}); λ_I is the constant that reflects the exchange of volume of water per unit of time (h^{-1}); C^*, ^{222}Rn concentration in recharge water using models (Bq·l^{-1}); C_R, ^{222}Rn concentration in recharge water using LSC (Bq·l^{-1}); L_D, detection limit of LSC is 2 Bq·l^{-1}.

with LSC. These results indicate that, although the model fits very well (the values of R^2 are very close to unity), it does not allow C^* to be correctly determined in the conditions of trials 2, 3 and 4.

Simulations 5, 6 and 7 were carried out with water rich in ^{222}Rn (which simulate the recharge of the aquifer with groundwater) and returned a higher value of C^* than the aquifer water, indicating that the recharge was carried out with deep waters rich in ^{222}Rn. However, the C^* values obtained in these three cases (696 ± 31; 673 ± 30; 812 ± 38 Bq·l^{-1}) are lower than C_R (2109 ± 88; 1805 ± 76; 2191 ± 91 Bq·l^{-1}).

The value of C^* (106 ± 17 Bq·l^{-1}) obtained with the model for the conditions of simulation 8 gives a better value than those obtained with the previous simulations, although it is still far from C_R.

The value of C^* (1924 ± 124 Bq·l^{-1}) obtained in simulation 9 is much higher than the concentration of the aquifer, clearly indicating that the recharge has occurred with groundwater, which is rich in ^{222}Rn. However, this value of C^* is far from C_R (3340 ± 136 Bq·l^{-1}).

Simulation 10 has provided a much better value of C^* (62 ± 23 Bq·l^{-1}) than the previous cases and is quite close to the value for public water (<2 Bq·l^{-1}).

The result of C^* (2020 ± 149 Bq·l^{-1}) in case 11, simulating a recharge with ^{222}Rn rich groundwater at constant volume of the aquifer, is still far from the real value (C_R) used during the recharge (3313 ± 135 Bq·l^{-1}). Nevertheless, it improves on the results of the previous simulations.

4. Discussion

A series of 11 recharge/discharge episodes in an artificial aquifer with ^{222}Rn in water have been simulated in the laboratory, reproducing natural processes such as recharge episodes with rainwater (where the ^{222}Rn concentration in water is lower than 2 Bq·l^{-1}) or with water from other aquifers (where the ^{222}Rn concentrations are high). In these simulations, volumes and times (and therefore flows) have been modified both in the recharge and discharge processes in order to analyse the behaviour of the Closed Compartment Model (CCM) and the Open Compartment Model (OCM).

After applying the mathematical model to the 11 episodes which were studied, we consider that for the OCM adjustment processes, 7–8 h of data after finishing the recharge process is sufficient to obtain good results. When CCM adjustments are made, more data is needed to reach equilibrium; in this study, between 250 and 300 h were needed.

The adjustments made to the experimental values, which were obtained in the simulated aquifer regarding the CCM and the OCM show very good R-squared values and are close to the unit.

The results of the model for the ^{222}Rn concentration in the recharge water (C^*) in the various recharge/discharge simulations, which were carried out in the artificial aquifer, provide different values from those expected. This situation happens when the volume of the artificial aquifer does not remain constant (simulations 2 to 9); i.e., when the recharge/discharge episodes are not simultaneous and have different flows. Despite these values, the results allow us to determine the origin of the water used in the recharge episodes, indicating whether water with a higher or lower ^{222}Rn concentration is present in the aquifer that has been used.

In the same way, the results obtained (in simulations 10 and 11) by the model in the artificial aquifer when the recharge/discharge episodes are carried out simultaneously and progressively (constant volume, which is a similar situation to the real case of Las Caldas Spa (Saínz et al., 2016)), are reasonably adjusted to the expected values.

5. Conclusions

The results of this study, together with previous ones (Saínz et al., 2016), indicate that this mathematical model (CCM and OCM) can be used when the volume of the aquifer is constant (when the recharge flow is similar to the discharge flow). The validation of the model carried out in this study with continuous measurements of ^{222}Rn in water will allow the concentration of ^{222}Rn in water to be used as a tracer to determine the origin and volume of water that feeds real aquifers such as thermal spas (facilities, where the water volumes are kept constant).

A future mathematical study will be necessary to adapt this model to

variable volumes of water in order to use it in all types of aquifers, but for now, this model at least permits to identify the origin of the water that reaches any type of aquifer.

In any case, the continuous monitoring of ^{222}Rn in water used in this study with an RTM 2100 with a specific continuous measurement system allows us to identify any change in the aquifer conditions in real time, if necessary.

Declaration of competing interest

The authors declare that they have no known competing financial interests or personal relationships that could have appeared to influence the work reported in this paper.

References

Avery, E., Bibby, R., Visser, A., Esser, B., Moran, J., 2018. Quantification of groundwater discharge in a subalpine stream using radon-222. Water 10, 100.

Celaya, G.S., 2018. Thesis: Study of ^{222}Rn Behavior in the Processes of Recharge-Discharge in Aquifers: Simulation in Laboratory and Application to a Real Case. University of Cantabria. https://repositorio.unican.es/xmlui/handle/10902/13308. 22/01/2018.

Celaya, G.S., Rábago, G.D., Fuente, M.I., Quindós, L., Bon Carreras, N., Valero Castell, M. T., Gutierrez Villanueva, J.L., Sainz Fernández, C., 2018a. A simple national intercomparison of radon in water radiation. Protect. Dosim. 181 (No. 4), 343–349.

Celaya, G.S., Fuente, M.I., Quindós, L., Sainz, F.C., 2018b. Optimization of a portable liquid scintillation counting device for determining ^{222}Rn in water. Radiat. Meas. 117, 1–6.

Cigna, A.A., 2005. Radon in caves. Int. J. Speleol. 34, 1–18. ISSN 0392-6672.

WHO Regional Office for Europe, Copenhagen, Denmark, 2001. WHO Air Quality Guidelines for Europe, second ed., pp. 1–14 (Chapter 8).3 Radon. 2001.

CSN, 2001. Proyecto Marna. Mapa 1:1000000 de radiación gamma natural. Ediciones del Consejo de Seguridad Nuclear, 2001. https://www.csn.es/documents/10182/2778 6/INT-04-02+Proyecto+Marna.+Mapa+de+radiaci%C3%B3n+gamma+natural.

Galán, L.M., Martín, S.A., Gómez, E.V., 2004. Application of ultra-low level liquid scintillation to the determination of ^{222}Rn in groundwater. J. Radioanal. Nucl. Chem. 261 (No 3), 631–636.

Haroon, H., Muhammad, S., 2022. Spatial distribution of radon concentrations in groundwater and annual exposure doses in Mirpur District Pakistan. Groundwater Sustain. Dev. 17 https://doi.org/10.1016/j.gsd.2022.100734. May 2022. Article number 100734.

ICRP Publication 137, 2017. Occupational Intakes of Radionuclides Part **3**, pp. 297–317. Chapter 12.

Kham, Qasim, Alshamsi, Dalal, Hussein, Saber, Mohamed, Mohamed, 2021. Understanding the activity of Radon-222 in a sand dune aquifer of an arid region through the application of machine learning. November Groundwater Sustain. Dev. 15. https://doi.org/10.1016/j.gsd.2021.100667. Article number 100667.

Kowalczk, A.J., Froelich, P.N., 2010. Cave air ventilation and CO_2 outgassing by radon-222 modeling: how fast do caves breathe? Earth Planet Sci. Lett. 289, 209–219.

Laboratoire National Henri Becquerel, 08 June, 2018. Nuclear Data-Laboratoire National Henri Becquerel. http://www.lnhb.fr/nuclides/Pb-214_tables.pdf.

Lario, J., Sánchez-Moral, S., Cuezva, S., Taborda, M., Soler, V., 2006. High ^{222}Rn levels in a show cave (Castañar de Ibor, Spain): proposal and application of management measures to minimize the effects on guides and visitors. Atmos. Environ. 40, 7395–7400.

Nero, A.V., Gadgil, A.J., Nazaroff, W.W., Revzan, K.L., 1990. Indoor Radon and Decay Products: Concentrations, Causes, and Control Strategies. Department of Civil engineering University of California Berkeley. Lawrence Berkeley Laboratory. University of California. Applied Science Division. LBL-27798. January 1990.

Quindós, L., 1995. Un gas radiactivo de origen natural en su casa. Universidad de Cantabria & Consejo de Seguridad Nuclear, 27/01/2020. http://elradon.com/radon -un-gas-radioactivo-de-origen-natural-en-su-casa.

Sainz, C., Rábago, D., Fuente, I., Celaya, S., Quindós, L.S., 2016. Description of the behavior of an aquifer by using continuous radon monitoring in a thermal spa. Sci. Total Environ. 543, 460–466.

Selvam, S., Muthukumar, P., Sajeev, S., Venkatramanan, S., Chung, S.Y., Brindha, K., Suresh Babu, D.S., Murugan, R., 2021. Quantification of submarine groundwater discharge (SGD) using radon, radium tracers and nutrient inputs in Punnakayal, south coast of India. Geosci. Front. 12, 29–38.

Veiga, L.H.S., Melo, V., Koifman, S., Amaral, E.C.S., 2004. High radon exposure in a Brazilian underground coal mine. J. Radiol. Prot. 24, 295–305.

Wisser, S., Frenzel, E., Dittmer, M., 2006. Innovative procedure for the determination of gross-alpha/gross-beta activities in drinking water. Appl. Radiat. Isot. 64, 368–372.

Youssef, M., Hanfi, M., 2019. Radiological assessment of gamma and radon dose rates at former uranium mining tunnels in Egypt. Environ. Earth Sci. 78, 113.